IOP Publishing Physiol. Meas. 39 (2018) 104001 (8pp) https://doi.org/10.1088/1361-6579/aae195

Physiological Measurement

IPEM Institute of Physics and Engineering in Medicine

PAPER

Effect of abdominal aortic endoprostheses on arterial pulse wave velocity in an *in vitro* abdominal aortic flow model

Kim van Noort[1,2,5], Suzanne Holewijn[3,6], Richte C L Schuurmann[2,4], Johannes T Boersen[1,2], Simon P Overeem[1,2], Erik Groot Jebbink[2,3], Jenske J M Vermeulen[2], Michel M P J Reijnen[3], Cornelis H Slump[2,5] and Jean-Paul P M de Vries[4]

[1] Department of Vascular Surgery, St. Antonius Hospital, Nieuwegein, Netherlands
[2] Multi-Modality Medical Imaging Group, Technical Medical Center, University of Twente, Enschede, Netherlands
[3] Department of Vascular Surgery, Rijnstate Hospital, Arnhem, Netherlands
[4] Department of Surgery, Division of Vascular Surgery, University Medical Centre Groningen, Groningen, Netherlands
[5] Robotics and Mechatronics, Faculty of Electrical Engineering, Mathematics, and Computer Science, University of Twente, 7500 AE, Enschede, The Netherlands
[6] Address of correspondence: Department of Surgery, Rijnstate Hospital, Wagnerlaan 55, PO Box 9555, 6800 TA, Arnhem, Netherlands

E-mail: sholewijn@rijnstate.nl

Keywords: pulse wave velocity, abdominal aorta aneurysm, endovascular aneurysm repair, endograft, structural stiffness

RECEIVED
28 May 2018

REVISED
5 September 2018

ACCEPTED FOR PUBLICATION
14 September 2018

PUBLISHED
11 October 2018

Abstract

Objective: Aortic pulse-wave-velocity (aPWV) is a measure for arterial stiffness, which is associated with increased cardiovascular risk. Recent evidence suggests aPWV increases after endograft-placement for aortic aneurysms. The aim of this study was to investigate the influence of different aortic endoprostheses on aPWV and structural stiffness *in vitro*. *Approach*: Three different abdominal aortic endoprostheses (AFX, Endurant II, and Nellix) were implanted in identical silicone aneurysm models. One model was left untreated, and another model contained an aortic tube graft (Gelweave). The models were placed in an *in vitro* flow set-up that mimics physiological flow. aPWV was measured as the transit time of the pressure wave over the flow trajectory of the suprarenal to iliac segment. Structural stiffness corrected for lumen diameter was calculated for each model. *Results*: aPWV was significantly lower for the control compared to the AFX, Endurant, Nellix and tube graft models (13.00 ± 1.20, 13.40 ± 1.17, 18.18 ± 1.20, 16.19 ± 1.25 and 15.41 ± 0.87 m s^{-1}, respectively ($P < 0.05$)). Structural stiffness of the AFX model was significant lower compared to the control model (4718 N m^{-1} versus 5115 N m^{-1} ($P < 0.001$), respectively), whereas all other models showed higher structural stiffness. *Significance*: Endograft placement resulted in a higher aPWV compared to a non-treated aortic flow model. All models showed increased structural stiffness over the flow trajectory compared to the control model, except for the AFX endoprosthesis. Future studies in patients treated with an endograft are needed to evaluate the current results *in vivo*.

Abbreviations

AAA	Abdominal aortic aneurysms
(a)PWV	(Aortic) pulse wave velocity
BMF	Blood mimicking fluid
CT	Computed tomography
EVAR	Endovascular aneurysm repair
PTFE	Polytetrafluoretheen

Introduction

Abdominal aortic aneurysms (AAA) have been associated with increased arterial wall stiffness, affecting the Windkessel function, which results in increased flow velocities and augmented pressure wave reflections [1–4]. Augmented pressure opposing the left ventricle ejection may lead to amplified aortic and ventricular pressures

during systole and reduced aortic pressure during diastole, which may result in decreased perfusion of the coronary arteries and discontinuous perfusion of peripheral tissue [5]. These effects have been associated with an increased risk for coronary heart disease, stroke and cardiovascular adverse events (hazard ratios 1.35, 1.54, and 1.45 respectively) [6].

Several studies report an increase in arterial stiffness after endovascular aneurysm repair (EVAR), derived from the arterial pulse wave velocity (aPWV) measured over the carotid to femoral artery trajectory or brachial to below-the-knee artery trajectory [7, 8, 10, 18–20]. It has been suggested that this increased stiffness post-EVAR is a risk factor for future cardiovascular adverse events. In some studies an increased aortic stiffness has been described within days or weeks after EVAR, suggesting that the endograft itself stiffens the aortic tract [8, 9].

However, aPWV is not only affected by changes in aortic stiffness. A decrease in vessel radius causes an increase in velocity if the flow is constant. Therefore the radius decrease due to implantation of the endoprosthesis needs to be included when calculating changes in aortic stiffness after EVAR [11, 12].

The aim of this study is to investigate the influence of three different aortic endoprostheses on aPWV over the aortoiliac trajectory *in vitro* by measuring the aPWV in an untreated AAA model, three different endograft models and a tube graft model, which is commonly used for open surgical reconstruction of the aorta. Moreover, a comparison is made between the structural stiffness over the flow trajectory for the different endograft models and the untreated AAA model.

Methods

Models

Five identical flexible silicone abdominal aortic aneurysm models were used (Shore-A40, Elastrat Sàrl, Geneva, Switzerland). Each model had the same dimensions, which were based on the average dimensions of 25 elective AAA patients: suprarenal aorta diameter of 26 mm, maximum aneurysm diameter of 50 mm and common iliac artery diameters of 12 mm (figure 1). One aneurysm model served as negative control. In three models, a commercially available endograft was placed: the AFX (Endologix, Irvine, CA, USA), Endurant II (Medtronic, Minneapolis, MN, USA), and Nellix (Endologix). All endografts were deployed according to the instructions for use by an experienced vascular surgeon (figure 2). A tube graft (Gelweave, Vascutec, Inchinnan, Renfrewshire, Scotland, UK), which is used in open surgical repair, was fixated in the fifth model.

Ideally, the same diameters for every configuration should have been used. However, the Endurant and AFX endografts are not available in the same dimensions when $>$29 mm. For proper oversizing compared to the flow model (29 mm) an Endurant 32 mm and an AFX 34 mm was selected. Moreover, the Nellix configuration is always 10 mm in diameter. All the configurations used are selected as the optimal configuration for the specific endograft in this models' anatomy.

The AFX unibody and limb diameters were 28 mm and 16 mm, respectively. The AFX suprarenal fixating aortic extension had a diameter of 34 mm with a length of 80 mm. Total length of the AFX configuration was 140 mm. The Endurant endograft main body and limb diameters were 32 mm and 16 mm, respectively. The total length of the Endurant configuration was 166 mm. The Nellix endosystem configuration consisted of two stent frames with a diameter of 10 mm and a length of 150 mm. The endografts were surrounded by endobags filled with 128 ml of polymer with a fill pressure of 180 mmHg to completely seal the aortic aneurysm and the landing zones in the common iliac arteries. The tube graft configuration had a diameter of 30 mm and a length of 100 mm. For securing of the tube graft into the silicone model, the tube graft was clamped at its proximal and distal ends to mimic an anastomosis.

In vitro flow setup

An in-house built circulatory system with physiological flow and pressure conditions (figure 3) was used [13]. The superior mesenteric artery and renal arteries were sealed off. The system included three parallel gear pumps (12 V, Kavan, type 0190.121; Kavan GmbH, Nürnberg, Germany) generating pulsatile flow with a mean flow of 1 l min^{-1} at 75 beats min^{-1}. Flow conditions were monitored with two flow sensors (UF08B, Cynergy3, Redondo Beach, CA, USA) at the outflow trajectory of the iliac arteries. The systemic pressure was set to a physiological range of 120/80 mmHg, continuously monitored with two pressure sensors (40PC015G1A, Honeywell, Morris Plains, NJ, USA). The pressure sensors were placed on fixed distances proximal and distal from the superior mesenteric artery branch (150 and 324 mm, respectively).

The trajectory length between the two pressure sensors was measured over a centerline through the center of the aortic lumen, created semi-automatically on a 3mensio workstation (Pie Medical, Maastricht, The Netherlands) based on high resolution computed tomography (CT) scans of the five models.

CT scans were acquired on a 512-slice CT scanner (Philips Healthcare, Eindhoven, the Netherlands). Scans acquisition parameters were: tube potential, 120 kV; tube current time product, 200 mAs; increment, 0.75 mm; pitch, 0.78; collimation, 125 $\times$ 0.625 mm and slice thickness, 0.9 mm.

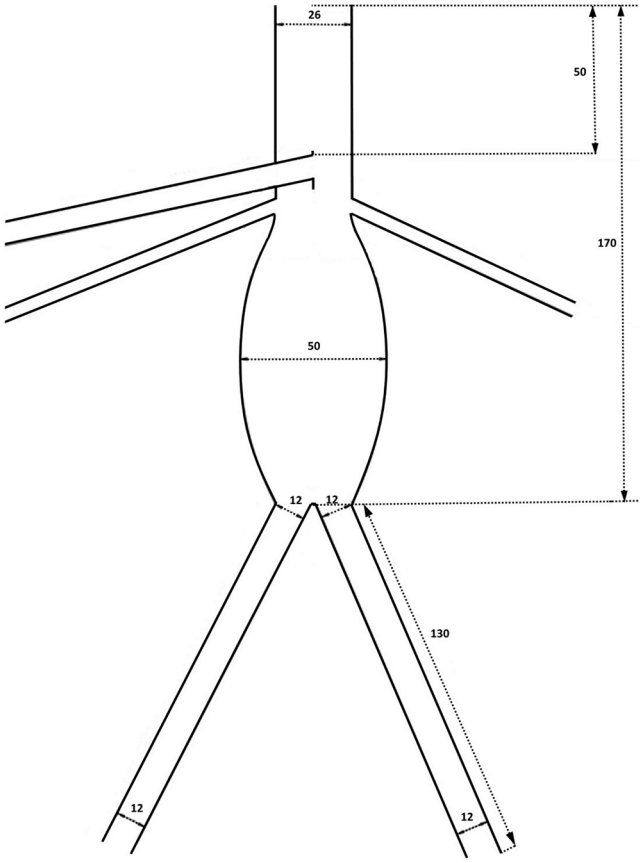

Figure 1. Schematic representation of the silicone abdominal aortic aneurysm model. Diameters are 26, 50 and 12 mm for the suprarenal aorta, infrarenal aorta and iliac arteries respectively. The silicon model had a total center luminal length of 300 mm from the proximal aorta end to the distal iliac end.

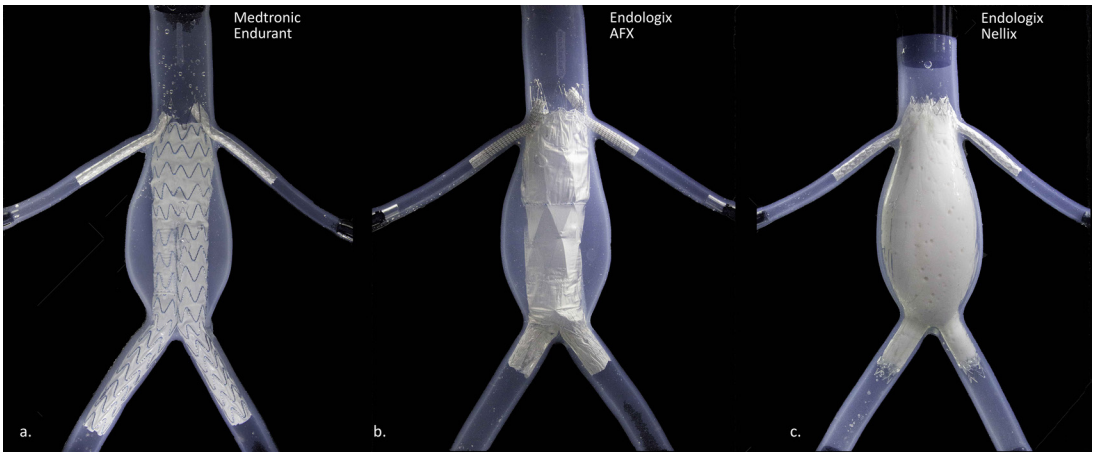

Figure 2. Identical silicone models with three commercially available endograft configurations implanted. (a) Endurant II—main body diameter 32 mm, limb diameters 16 mm, total length 166 mm; (b) AFX—main body diameter 34 mm, unibody diameter 28 mm, limb diameters 16 mm, total length 140 mm; (c) Nellix—stent frame diameter 10 mm, length 150 mm, endobags were filled with 128 ml of polymer. Each model was equipped with two self-expandable grafts (Viabahn, W.L. Gore and Associates, Flagstaff AZ) as part of a previous study. Since the renal branches were occluded, these stents have minor influence on the results of this study.

The mean flow radius of each model was measured on the created centerline, by measuring the radius every 5 mm over the trajectory length. The radius over the iliac trajectory is the sum of radii of the iliac arteries at 5 mm intervals.

One compliance chamber was added proximally and two distally of the aneurysm model, to simulate the vascular compliance (± 20 ml mmHg^{-1}), and peripheral resistance was controlled with needle valves at the outflow trajectory to ensure mean arterial pressure within physiological range. The blood mimicking fluid (BMF) that was pumped through the system had the viscosity of human blood (4.31 ± 0.03 cP) [14]. Sensors and fluid levels

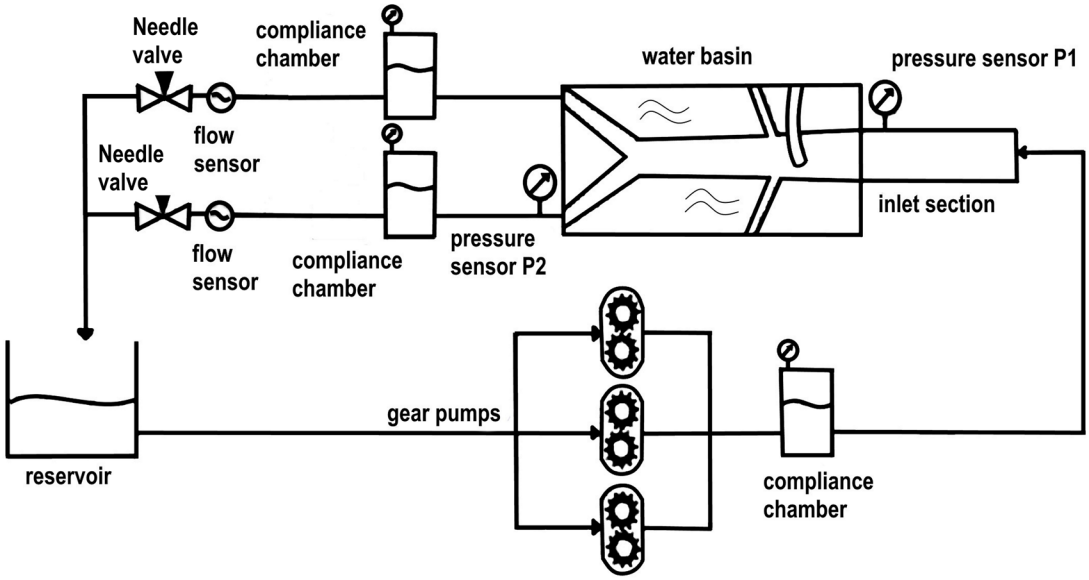

Figure 3. Schematic representation of the *in vitro* flow model set-up [13]. Physiological flow is simulated by generating a pulsatile flow with the gear pumps. The compliance chambers mimic arterial compliance. Flow is measured with flow sensors at the outflow of the set-up. Pressure waves are measured with pressure sensors P1 and P2. Pulse wave propagation time between P1 and P2 is calculated. An abdominal environment of 5–7 mmHg was simulated by surrounding the models with 6 liters of water in a basin. Pulse wave velocity (PWV) over the *in vitro* aortic trajectory is measured as the wave propagation time divided by the distance between P1 and P2.

in the compliance chambers were calibrated and adjusted if needed when the silicone models were switched to ensure comparable flow and pressure conditions of the system. An abdominal environment of 5–7 mmHg was simulated by surrounding the models with 6 liters of water (67–95 mmH_2O) to mimic the abdominal pressure on the aorta (figure 3) [15].

Pressure measurement

Data was analyzed using Matlab 2015B (MathWorks, Natick, USA). Before pressure measurements were performed, the system was calibrated by applying a constant flow of 500 ml min^{-1} per iliac artery. During constant flow, remaining air was flushed out of the system, and the digital pressure sensors were calibrated with an analogous pressure sensor that was connected to the suprarenal inflow pipe. Each pressure measurement consists of two consecutive pressure profiles. These measurements were performed ten times, resulting in 20 pressure profiles. To investigate the variation of the setup, the measurements were repeated seven times over 2 d for the control, AFX, Endurant, and Nellix models. The system was dismounted and remounted between the measurement days. The same fluid was used both days.

Stiffness measurements

Pulse wave velocity

The aPWV was calculated as the velocity of the pulse wave propagating over the trajectory length during the transit time. The pressure profiles at the locations of the fixed proximal and distal pressure sensor locations were continuously recorded over two cardiac cycles during 1.6 s with a sample frequency of 1.22 kHz.

The transit time, the duration over which the pressure propagates between the two pressure sensors, was calculated with the foot-to-foot method. This is the same method applied in the SphygmoCor system (AtCor Medical, Sydney, Australia), which is commonly used to measure aPWV in patients. It is defined as the time between the onset of the pressure buildup of the proximal pressure sensor to the onset of the pressure buildup of the distal pressure sensor. This foot-to-foot method was found to be reproducible for calculating aPWV in rat models and showed only minor influence of wave reflections [16]. High frequency noise (>61 Hz) was removed from the data.

Structural stiffness

The aPWV is calculated with the Moens–Korteweg equation and is affected by the stiffness and the mean radius of the flow trajectory (equation (1)):

$$\mathrm{aPWV} = \sqrt{\frac{E_{inc}h}{2r\rho}} \tag{1}$$

Table 1. Mean and standard deviation of aPWV for the control, AFX, Endurant, and Nellix models measured on day 1 and day 2. A total of 140 pulse waves were analyzed for each model, divided over 60 and 80 times per day.

	Day 1			Day 2		
Models	*N*	Mean aPWV (m s^{-1})	SD (m s^{-1})	N	Mean aPWV (m s^{-1})	SD (m s^{-1})
Control	59	12.93	1.19	80	13.05	1.21
AFX[a]	80	12.97	0.93	60	13.98	1.23
Endurant	60	18.33	1.26	80	18.07	1.15
Nellix[a]	79	15.62	1.06	59	16.96	1.07

Note: Mean and standard deviation are given in m s^{-1}. *N* is the amount of pulse waves analyzed.
[a] Significant difference in aPWV between day 1 and day 2 ($P < 0.001$).

where $E_{inc}h$ is the structural stiffness over the flow trajectory (N m^{-1}), aPWV the pulse wave velocity over the flow trajectory (m s^{-1}), r the mean trajectory radius (m) and ρ the fluid density (kg m^{-3}). The structural stiffness over the flow trajectory is a combination of the incremental Young's modulus (E_{inc}) and the wall thickness (h) of the silicon models [11, 12]. According to equation (1), change in the mean trajectory radius r with the same aPWV and fluid density ρ results in a change in stiffness. The stiffness over the flow trajectory for all silicone models mimicked the physiologic compliance of the aorta wall in AAA patients [7]. Since the material properties were equal for all silicone models, differences in measured stiffness over the flow trajectory were the result of different endograft configurations in the models.

Statistical analysis

The Shapiro–Wilk test was performed to assess normal distribution of the data. The data was normally distributed and is presented as mean with standard deviation. Paired samples *t*-tests and analyses of variance (ANOVA) with repeated measures design were performed to compare the different aPWV's per day and between measurement days, including Bonferoni correction for multiple testing. Differences in aPWV and structural stiffness between the control model and endograft models were tested using independent samples *t*-tests. The variance of the total set of measurements was determined for each model by the coefficient of variation (standard deviation/average), and significance of variation differences between the groups was tested with Levene's test. *P*-values <0.05 (two-tailed) were considered significant. Analyses were performed using SPSS, IBM 24.0 software (IBM Corp, Armonk, NY, USA).

Results

The trajectory length over the centerline between the two pressure sensors was 474 mm for all models. Mean radius of the models over the trajectory length between the two pressure sensors was 13.5 mm, 11.7 mm, 12.1 mm, 10.4 mm and 11.8 mm for the control, AFX, Endurant, Nellix and tube grafts models, respectively.

Table 1 shows the mean aPWV and standard deviation of measurements performed on day one and day two for the control, AFX, Endurant and Nellix models. aPWV in the AFX and Nellix models were significantly different between the 2 d, in contrast to the control and Endurant measurements, which were similar on both measurement days.

Table 2 shows the results of the mean aPWV of all measurements on both days, the model stiffness not corrected for the average diameter, and the structural stiffness corrected for average diameter of all models. The aPWV as well as the structural stiffness over the flow trajectory of all endograft models and the tube graft are significantly different compared to the control model. The structural stiffness over the flow trajectory of the AFX model is significant lower compared to the control model (4718 N m^{-1} versus 5115 N m^{-1} ($P < 0.001$), respectively), while the other models have a significantly higher stiffness than the control model ($P < 0.001$).

Changes of the aortic diameter due to deployment of the (endo)grafts led to a decrease of the structural stiffness over the flow trajectory of 13%, 11%, 23% and 13% for the AFX, Endurant, Nellix and tube graft models, respectively, compared to measurements not adjusting for diameter change.

The coefficients of variation of the measurements were 9.2%, 8.8%, 6.6% and 7.7% for the control, AFX, Endurant, and Nellix models, respectively. Levene's test of variance showed no significant differences in variance between groups ($p = 0.802$).

Discussion

The results of this *in vitro* study show an increase in aPWV for all endoprostheses models compared to the control model. However, the structural stiffness over the flow trajectory was reduced in the AFX model compared with the control model, in contrast to the other devices. This is likely related to the AFX design, where

Table 2. Mean aPWV, standard deviation and structural stiffness over the flow trajectory with and without correction for the graft diameter.

Models	Mean aPWV ($m\ s^{-1}$)	Structural stiffness over flow trajectory not corrected for graft diameter ($N\ m^{-1}$)	Actual structural stiffness over flow trajectory ($N\ m^{-1}$)
Control	13.00 ± 1.20	5115 ± 966	5115 ± 966
AFX[a]	13.40 ± 1.17[b]	5433 ± 966[c]	4718 ± 839[d]
Endurant[a]	18.18 ± 1.20[c]	9966 ± 1333[c]	8919 ± 1193[c]
Nellix[a]	16.19 ± 1.25[c]	7918 ± 1224[c]	6128 ± 947[c]
Tube graft[a]	15.41 ± 0.87[c]	7148 ± 774[c]	6241 ± 676[c]

[a] Models differ significantly from the control model in mean aPWV, structural stiffness over the flow trajectory not corrected and corrected for graft diameter with a *P*-value.
[b] *P*-value of 0.005.
[c] *P*-value of <0.001.
[d] *P*-value of 0.006.

the polytetrafluoretheen (PTFE) of the AFX is situated outside the endoskeleton and is only attached to the proximal and distal ends of the endoskeleton, in contrast to other EVAR grafts that have an exoskeleton. One could hypothesize that this would lead to other wave reflection patterns (better propagation of the pulse waves) compared to other endografts and thereby reducing cardiac load. Whether this has clinical consequences, in terms of improved cardiovascular outcomes, needs to be further investigated *in vivo*.

Interestingly, the highest aPWV was expected in the Nellix model, due to the large decrease in trajectory diameter (no main body, but two 10 mm diameter stent frames, resulting in more proximal neo-bifurcation), and the balloon expandable stent frames. However, only a modest increase in aPWV and structural stiffness over the flow trajectory was observed. One explanation might be the elastic characteristics of the polymer used in the Nellix endobags. The pressure of the pulse wave might have been damped by the polymer, resulting in only a slight increase in aPWV despite the large decrease in trajectory diameter.

So far limited and conflicting evidence is available on the relation between aPWV and AAA. Some studies showed an increased aPWV [7, 10], whereas others showed decreased aPWV in untreated AAA patients [9, 17]. Most studies using tonometry were performed in relatively small sample sizes. Furthermore, studies have convincingly shown that aPWV increases after EVAR [7, 8, 10, 18–20]. Pre- and post-EVAR velocities of respectively 13.11 ± 3.57 and $16.41 \pm 2.33\ m\ s^{-1}$ have been described in the literature. In contrast, normal values for aPWV, are 9.7 (5.7–13.6) $m\ s^{-1}$ and increase with age [21]. These post EVAR values are comparable to the results of this *in vitro* study.

A meta-analysis of Ben-Shlomo *et al* [6] showed that a change of aPWV of $1\ m\ s^{-1}$ was associated with a hazard ratio for cardiovascular events of 1.07 (95% CI 1.02–1.12 weighted mean and standard deviation of 10.1 and $3.3\ m\ s^{-1}$, respectively) for a male aged 60 years (non-smoker, non-diabetic, no blood pressure medication, systolic blood pressure of 120 mmHg, total cholesterol $5.5\ mmol\ l^{-1}$, and HDL cholesterol of $1.3\ mmol\ l^{-1}$). We may conclude that the increase in aPWV determined in the current *in vitro* study due to endograft placement will be clinically relevant. However, while the transit time over the stented trajectory is reduced, velocity over the unstented areas is probably not affected post-EVAR. Since the total carotid-femoral pathway is longer than modeled in this study, average aPWV over the total pathway may be slightly lower *in vivo*.

It is therefore important to design an endograft which has minimal influence on the aPWV. To do so, diameter and stiffness of the endograft need to be considered.

A recent study reported differential effects of endograft fabric types on aPWV. Both PTFE and polyesther grafts resulted in increased aPWV post-implant compared to pre-implant but polyesther grafts showed the largest increase. The authors suggested the inflammatory response after EVAR and differences in stent graft design as potential explanations for the increased aPWV [22].

Comparison of studies is limited because of the use of different devices. Another limitation mentioned is that a large variation in stiffness parameters is reported. Furthermore, studies relating aPWV to outcome in patients treated with EVAR are lacking. What needs to be investigated is if the increase in aPWV after EVAR contributes to the increased cardiovascular risk in AAA patients. What also remains to be elucidated is if pulse wave analysis measurements, that provide measurements of wave reflection and cardiac output, provide reliable results in untreated and treated AAA patients. The ongoing ABC-study will provide the first results (NCT03469388).

Gray *et al* [23] showed a decrease in aPWV after open repair, whereas in this *in vitro* study an increase in aPWV in the tube graft was observed. One explanation might be that the tube graft has been clamped in the abdominal aortic model, whereas in real-life an aortotomy is performed and the tube graft is not surrounded by an intact aneurysm. In both studies a Gelweave tube graft was used.

The *in vivo* studies on aPWV and arterial stiffness use aPWV as a measure for arterial stiffness. However, this study shows the importance of correcting for the radius of the measured trajectory before comments on arterial stiffness and changes in arterial stiffness can be made. Endograft placement changes the stiffness of the flow trajectory, however the amount of change in stiffness depends not only on the design of the endograft but also on the diameter change after EVAR. For the effect on cardiac events, it may not be relevant if aPWV is increased due to increased stiffness or reduced diameter, but as both lumen diameter and material properties of the endograft affect the PWV, manufacturers should consider both in their stent design. An increase in structural stiffness and thus aPWV may result in an increased risk for coronary heart disease, stroke and cardiovascular disease [6].

This study has several limitations. First, this is an *in vitro* study. The main focus of this study was to determine eventual difference between endograft configurations in an aneurysm model and therefore a non-aneurysmatic aorta model was not included and an untreated AAA model was used as control. This study did not include the eventual effect of mural thrombus and calcifications, which may be of influence on aPWV *in vivo*. Therefore, results cannot be extrapolated 1:1 to clinical outcomes. However, the silicone models were designed with a physiologic compliance [13]. Moreover, these results may be more reliable than aPWV and structural stiffness measurements *in vivo* for comparison of different endografts on stiffness. The conditions in this set-up where controllable and could be measured easily, while conditions such as blood pressure, arterial compliance, flow diameter and trajectory length are much harder to control and measure *in vivo* [24]. Second, there are small (and some significant) changes in aPWV between the measurement days. These changes are possibly a result of changes in the model settings. Slightly less filling of the compliance chambers or air in the system may result in changes in aPWV. To avoid this, the model is calibrated before performing the aPWV measurements. We also checked for trends in aPWV across measurements, we could not detect a trend for decline or increase in aPWV over time.

Conclusion

Endograft placement resulted in a higher aPWV compared to a non-treated aortic flow model. The AFX endoprosthesis showed a decrease in structural stiffness compared to the control model over the flow trajectory. When calculating stiffness based on aPWV, change in diameter needed to be considered to avoid overestimation of the stiffness. Future studies should be performed in patients treated with an endograft to evaluate the current results *in vivo*.

ORCID iDs

Suzanne Holewijn https://orcid.org/0000-0001-7641-1322

References

[1] He C M and Roach M R 1994 The composition and mechanical properties of abdominal aortic aneurysms *J. Vasc. Surg.* **20** 6–13
[2] Kadoglou N P E *et al* 2012 Arterial stiffness and novel biomarkers in patients with abdominal aortic aneurysms *Regul. Pept.* **179** 50–4
[3] MacSweeney S T R, Young G, Greenhalgh R M and Powell J T 1992 Mechanical properties of the aneurysmal aorta *Br. J. Surg.* **79** 1281–4
[4] Durmus I, Kazaz Z, Altun G and Cansu A 2014 Augmentation index and aortic pulse wave velocity in patients with abdominal aortic aneurysms *Int. J. Clin. Exp. Med.* **7** 421–5
[5] London G M and Pannier B 2010 Arterial functions: how to interpret the complex physiology *Nephrol. Dial. Transplant.* **25** 3815–23
[6] Ben-Shlomo Y *et al* 2010 Aortic pulse wave velocity improves cardiovascular event prediction: an individual participant meta-analysis of prospective observational data from 17 635 subjects *J. Am. Coll. Cardiol.* **63** 636–46
[7] Kadoglou N P E *et al* 2012 Changes in aortic pulse wave velocity of patients undergoing endovascular repair of abdominal aortic aneurysms *J. Endovasc. Ther.* **19** 661–6
[8] Takeda Y *et al* 2014 Endovascular aortic repair increases vascular stiffness and alters cardiac structure and function *Circ. J.* **78** 322–8
[9] Lee C W *et al* 2013 Measures of carotid-femoral pulse wave velocity and augmentation index are not reliable in patients with abdominal aortic aneurysm *J. Hypertens.* **31** 1853–60
[10] Lantelme P, Mestre C, Lievre M, Gressard A and Milon H 2002 Heart rate: an important confounder of pulse wave velocity assessment *Hypertension* **39** 1083–7
[11] Tijsseling A S, Anderson A A, Moens I and Korteweg D J 2003 On the speed of propagation of waves in elastic tubes *Conf. on Pressure Surges* (BHR Group) pp 1–19 (http://www.win.tue.nl/~atijssel/pdf_files/CASA-12-42.pdf)
[12] Gosling R G and Budge M M 2003 Terminology for describing the elastic behavior of arteries *Hypertension* **41** 1180–2
[13] Groot Jebbink E *et al* 2016 Hemodynamic comparison of stent configurations used for aortoiliac occlusive disease *J. Vasc. Surg.* **66** 251–60
[14] Yousif M Y, Holdsworth D W and Poepping T L 2010 A blood-mimicking fluid for particle image velocimetry with silicone vascular models *Exp. Fluids* **50** 769–74
[15] Cheatham M L *et al* 2007 Results from the international conference of experts on intra-abdominal hypertension and abdominal compartment syndrome. II. Recommendations *Intensive Care Med.* **33** 951–62
[16] Mitchell G F, Pfeffer M A, Finn P V and Pfeffer J M 1997 Comparison of techniques for measuring pulse-wave velocity in the rat *J. Appl. Physiol.* **82** 203–10
[17] Bailey M A *et al* 2014 Carotid-femoral pulse wave velocity is negatively correlated with aortic diameter *Hypertens. Res.* **37** 926–32

[18] Paraskevas K I et al 2009 Evaluation of aortic stiffness (aortic pulse-wave velocity) before and after elective abdominal aortic aneurysm repair procedures: a pilot study *Open Cardiovasc. Med. J.* **3** 173–5
[19] Iwahashi T, Obitsu Y, Koizumi N, Shiraishi Y and Shigematsu H 2009 Clinical comparison of two different types of bifurcated graft for postoperative baPWV and ABI *Int. Angiol.* **28** 232–7
[20] Sekhri A R, Lees W R and Adiseshiah M 2004 Measurement of aortic compliance in abdominal aortic aneurysms before and after open and endoluminal repair: preliminary results *J. Endovasc. Ther.* **11** 472–82
[21] The Reference Values for Arterial Stiffness Collaboration 2010 Determinants of pulse wave velocity in healthy people and in the presence of cardiovascular risk factors: establishing normal and reference values *Eur. Heart J.* **31** 2338–50
[22] Kadoglou N P E et al 2014 Differential effects of stent-graft fabrics on arterial stiffness in patients undergoing endovascular aneurysm repair *J. Endovasc. Ther.* **21** 850–8
[23] Gray C, Goodman P, Badger S A, OMalley M K, ODonohoe M K and McDonnell C O 2016 Endovascular aneurysm repair increases aortic arterial stiffness when compared to open repair of abdominal aortic aneurysms *Vasc. Endovasc. Surg.* **50** 317–20
[24] Laurent S et al 2006 Expert consensus document on arterial stiffness: methodological issues and clinical applications *Eur. Heart J.* **27** 2588–605